ISSN 0016-7932, Geomagnetism and Aeronomy, 2020, Vol. 60, No. 7, pp. 929–935. © Pleiades Publishing, Ltd., 2020.

Energetics of X-Class Flares at the Minima of 22, 23, and 24 Solar Cycles

G. G. Motorina[a, b, *], A. L. Lysenko[c, **], S. A. Anfinogentov[d, *], and G. D. Fleishman[e, ****]**

[a]*Central Astronomical Observatory at Pulkovo of Russian Academy of Sciences, St. Petersburg 196140, Russia*

[b]*Astronomical Institute of the Czech Academy of Sciences, Ondřejov, Czech Republic*

[c]*Ioffe Institute, Polytekhnicheskaya, 26, St. Petersburg 194021, Russia*

[d]*Institute of Solar-Terrestrial Physics SB RAS, Lermontov St. 126, Irkutsk, 664033, Russia*

[e]*Center for Solar–Terrestrial Research, New Jersey Institute of Technology, University Heights, Newark, NJ 07102-1982, USA*

**e-mail: galina.motorina@asu.cas.cz*

***e-mail: alexandra.lysenko@mail.ioffe.ru*

****e-mail: anfinogentov@iszf.irk.ru*

*****e-mail: gfleishm@njit.edu*

Received March 4, 2020; revised March 10, 2020; accepted April 29, 2020

Abstract—Quite often powerful flares occur during a decrease of solar activity. In this work, we make an attempt to consider X-class flares at the minima of solar activity cycles as a separate group of events. Out of nine X-class flares we selected three such events that occurred at the minima of solar cycles 22–24: SOL1996-07-09T-09:09 (X2.6), SOL2006-12-13T-10:26 (X3.4), and SOL2017-09-06T-11:53 (X9.3); they were well observed by various instruments. All three selected flares are characterized by significant gamma-ray emission, which indicates ion acceleration during the impulsive phase. For the selected events, we estimated the energetics and distribution of the released free energy of the magnetic field between different flare components, including thermal energy and the energy of accelerated electrons and ions. No preferred energy-release channels have been identified for the considered flares at the solar activity minima. It turned out that the amount of magnetic free energy is several times higher than the amount of thermal energy and the energy of accelerated electrons and ions; the possible causes of this imbalance are discussed.

DOI: 10.1134/S001679322007018X

1. INTRODUCTION

Solar activity has a periodicity on different time scales from ~158 days to millennia (Solanki et al., 2004). One of the most pronounced solar-activity (SA) cycles is the 11-year cycle (Schwabe cycle), which manifests itself in changes in the international sunspot number (Wolf number), the total solar irradiance (TSI), the magnetic field, and other SA indices. A retrospective analysis of SA has showed that there was a sharp short-term SA increase during the minima of cycles 18–24, which was accompanied by powerful flares, namely, the flare of February 23, 1956, during the decay phase of cycle 18 (Meyer et al., 1956), the events of May 23–27, 1967, during the decay phase of cycle 19 (Knipp et al., 2016), the powerful flares during the minima of cycles 20–23 (Hathaway, 2015), and the flares of September 6, 7, and 10, 2017 (e.g., Yang et al., 2017, Omodei et al., 2018, Gary et al., 2018, Lysenko et al., 2019).

The number of solar-flare occurrences well correlates with the sunspot number and other activity indicators. However, active regions producing powerful solar flares can appear in any phase of the cycle, including the minima. The emergence of such active regions and the associated occurrence of powerful X-class flares was observed during the decay phase of solar cycles 21–24. It is possible that X-class flares occurred also at the minima of previous cycles, but the classification of events by X-ray classes by the GOES instruments (White et al., 2005) has become available only since 1975.

It appears that these events may be different from other flares; they are local maxima in the SA minima and constitute a separate group of events. There is a large number of works (Kosovichev and Zharkova, 1998; Mewaldt et al., 2009) devoted to X-class flares at solar minima. However, no joint analysis of events that occurred during the decay phase of different cycles has been conducted. The aim of this article is to estimate the thermal, nonthermal, and magnetic energies of X-class flares in the minima of SA cycles 22–24.

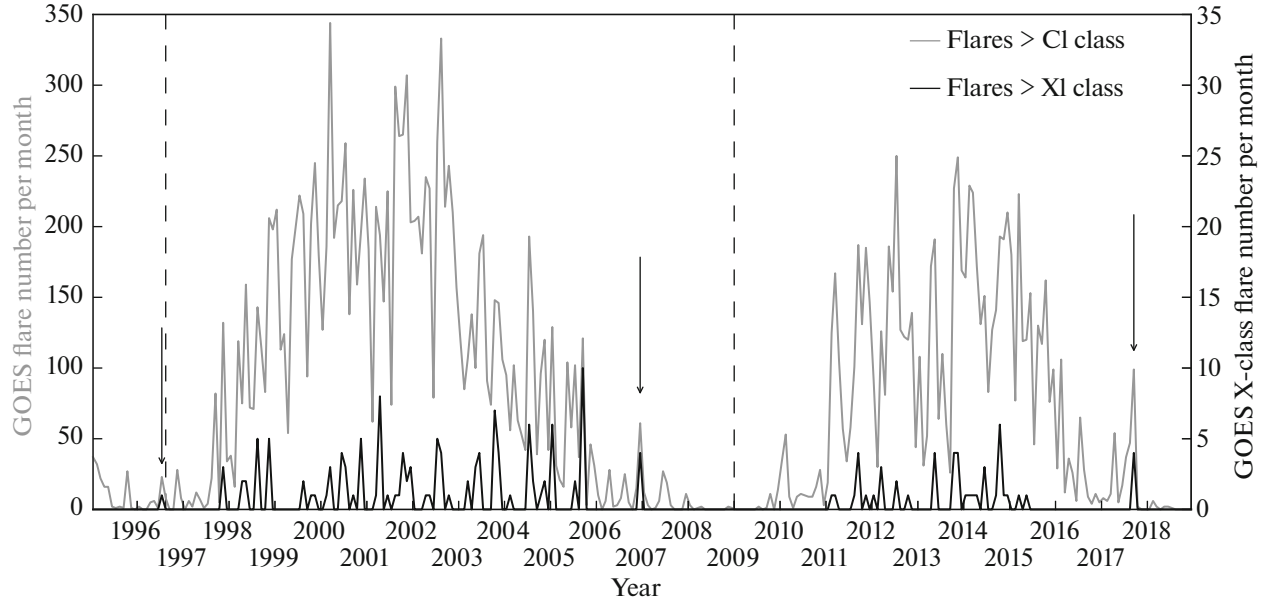

Fig. 1. Number of >C1-class (left scale, grey line) and >X-class (right scale, black line) solar flares for the minima of solar cycles 22–24 according to GOES. The arrows indicate the time when the studied X-class flares occurred.

2. INSTRUMENTATION AND EVENT SELECTION

Figure 1 shows the total number of >C1-class flares and the number of X-class flares according to GOES; the SA spikes considered in the article are marked with arrows. In 1996, 2006, and 2017, the Konus-Wind instrument (KW) (Aptekar et al., 1995) detected nine X-class events, which positions on the solar disk are shown in Fig. 2. Among these flares we chose the solar flares that were close to the disk center (in order to have magnetograms taken shortly before or shortly after the flare) and were well observed by other instruments. Three events were selected: SOL1996-07-09T-09:09 (X2.6), SOL2006-12-13T-10:26 (X3.4), and SOL2017-09-06T-11:53 (X9.3) (Fig. 2).

Soft (SXR) and hard X-ray (HXR), and gamma-ray (GR) flare data, as well as magnetograms of the active region taken close to the time of the flare occurrence, are required to estimate the thermal, nonthermal, and magnetic energy. For flares in the minima of cycles 22—24, there are HXR and GR data obtained by the KW instrument, which performs observations since 1994 in the range of ~15 keV–15 MeV, and for the last two minima the RHESSI data are available (Lin et al., 2002) in the energy range from ~3 keV to ~17 MeV. These data are used to estimate the nonthermal energy of accelerated electrons and ions. Figure 3 shows the light curves for the three selected flares obtained with the KW and RHESSI instruments.

The data obtained by GOES, which detects SXR in channels 1–8 Å and 0.5–4 Å, were used to estimate the thermal energy.

3. ESTIMATION OF SOLAR FLARE ENERGY

3.1. Thermal Energy

For estimation of the thermal energy emitted in SXR the method described by Emslie et al. (2012) was used. The total plasma energy emitted in the SXR range can be represented as $T\text{-}rad = EM \times Q(T)$, where $Q(T)$ is the radiative loss function (Raymond et al., 1976, the link to the rad_loss.pro function: http://www.chiantidatabase.org/tech_reports/09_rad_loss/chianti_report_09.pdf), EM is the emission measure, and T is the temperature, which were determined from the GOES data (Fig. 4). The duration of the flare (integration time) for which *T-rad* was found corresponds to the interval from the beginning of the flare recording by GOES to the time at which the radiation flux in channel 1–8 Å is reduced to 10% of the maximum value of the flux. Therefore, the following values were obtained for SOL1996-07-09T-09:09 (integration time: 0905–0925 UT) $T\text{-}rad = 2.02 \times 10^{30}$ erg, for SOL2006-12-13T-10:26 (0214–0346 UT) $T\text{-}rad = 15.3 \times 10^{30}$ erg, for SOL2017-09-06T-11:53 (1153–1340:45 UT) $T\text{-}rad = 25.9 \times 10^{30}$ erg (Table 1).

3.2. Energy of Accelerated Electrons

For energy estimation of the accelerated electrons the KW and RHESSI data (where available) were fitted using different modifications of the thick-target model with the OSPEX software package (https://hesperia.gsfc.nasa.gov/rhessi3/software/spectroscopy/spectral-analysis-oftware/index.html) (Brown, 1971; Syrovatskii and Shmeleva, 1972). The total energy of

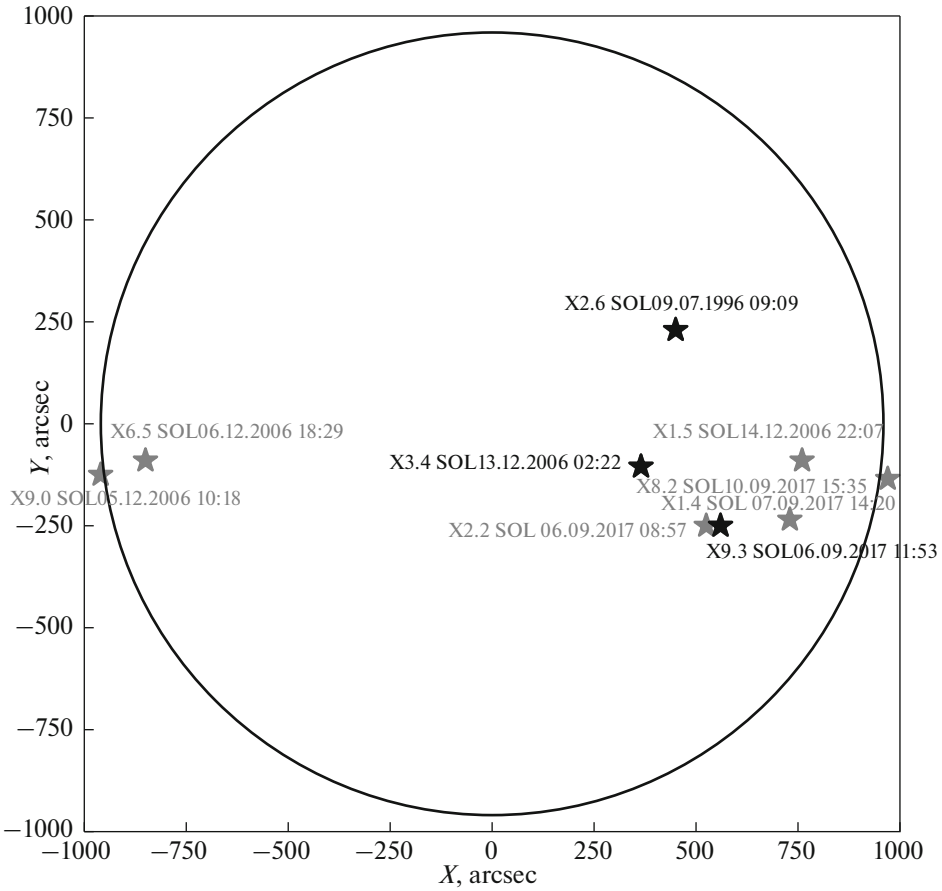

Fig. 2. Position of nine solar flares observed by KW in the triggered mode on the solar disk during the minima of SA cycles 22–24. The three solar flares selected for the analysis are marked in black.

the accelerated electrons was estimated as the sum of the obtained energy for each interval.

The KW spectra of the SOL1996-07-09T09:09 flare were fitted by the thick-target model, which implies a broken power-law spectrum of accelerated electrons characterized by two spectral indices—at lower and higher energies. The RHESSI data, with a correspondingly subtracted background available for the 2017-09-06T11:53 flare, were fitted by a two-component model, which includes an isothermal component and the thick-target model (Brown, 1971; Syrovatskii and Shmeleva, 1972). The KW data were fitted by a thick-target model that takes into account the return current (Zharkova and Gordovskyy, 2005).

Figure 5 shows the temporal evolution of the fitting parameters of the KW and RHESSI data for the SOL1996-07-09T-09:09 and SOL2017-09-06T-11:53 flares: total integral electron flux F_0 [10^{35} electrons s^{-1}], low-energy cut-off E_c [keV], and spectral index δ of the electron distribution function. Table 1 shows the

Table 1. Energy of X-class flares during SA minima

Solar flare	SOL1996-07-09T-09:09 (X2.6)	SOL2006-12-13T-10:26 (X3.4)	SOL2017-09-06T-11:53 (X9.3)
Free magnetic energy (E_{magn}), $\times 10^{30}$ erg	–	110	560
Thermal energy (*T-rad*), $\times 10^{30}$ erg	2.02	15.3	25.9
Energy of accelerated electrons (*E-elec*), $\times 10^{30}$ erg	30	13	84
Energy of accelerated ions (*E-ion*), $\times 10^{30}$ erg	10	14	11

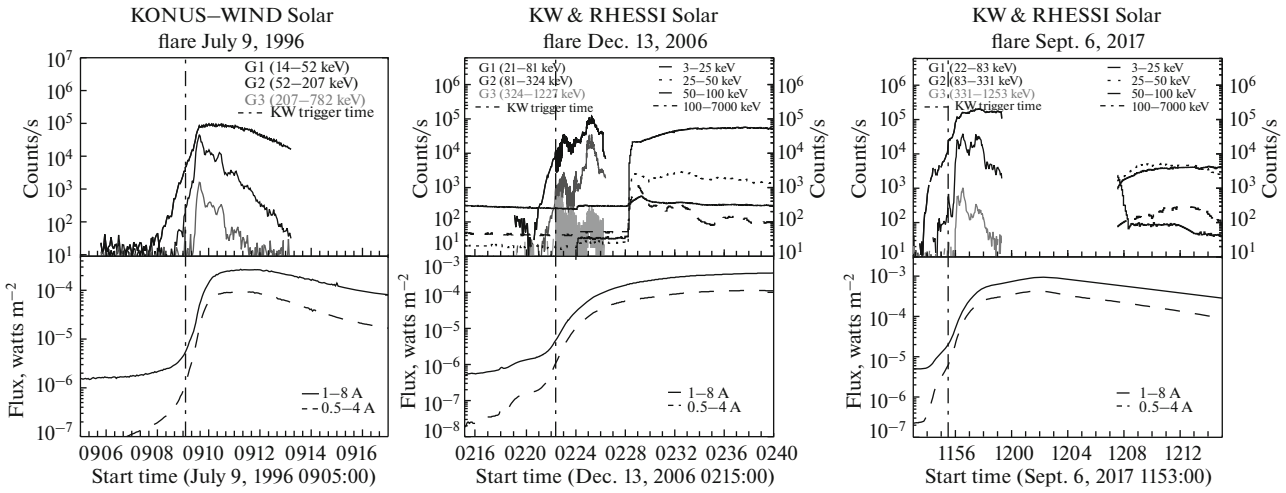

Fig. 3. HXR and GR time profiles in three channels according to KW (top panel, left scale) and RHESSI (top panel, right scale) data, SXR time profiles according to GOES (bottom panel) for the events SOL1996-07-09T-09:09 (X2.6) (left panel), SOL2006-12-13T-10:26 (X3.4) (middle panel), and SOL2017-09-06T-11:53 (X9.3) (right panel). The vertical dot-dash line shows the KW trigger time.

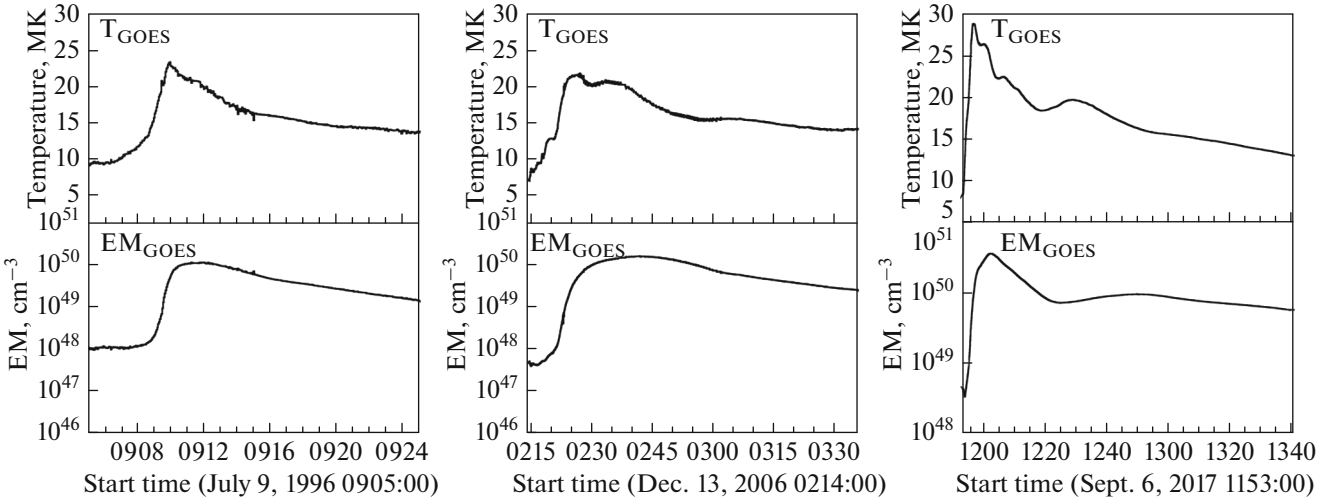

Fig. 4. Time profiles of temperature (top panel) and emission measure (bottom panel) according to GOES for the three selected events, as in Fig. 3.

energy values of nonthermal electrons for the flare on July 9, 1996 ($E\text{-}elec = 30 \times 10^{30}$ erg according to KW), December 13, 2006 ($E\text{-}elec = 13 \times 10^{30}$ erg, Emslie et al., 2012), and September 6, 2017 ($E\text{-}elec = 24 \times 10^{30}$ erg according to KW and $E\text{-}elec = 60 \times 10^{30}$ according to RHESSI). It should be noted that RHESSI and KW recorded about 2/3 of the flare on September 6, 2017 (Fig. 3, right panel). Therefore, the obtained estimates of the energy of accelerated electrons are only the lower limit.

3.3. Energy of Accelerated Ions

Significant emission at energies of >1 MeV was observed for the SOL1996-07-09T-09:09 and SOL2017-09-06T-11:53 flares. In addition to the bremsstrahlung continuum formed by accelerated electrons, the emission in this region is caused by nuclear reactions of accelerated in flares ions (Ramaty et al., 1975; Vilmer et al., 2011); thus, spectrum fitting in the gamma region makes it possible to estimate the characteristics of accelerated ions.

As a result of nuclear reactions excited nuclei are formed, and their transitions to the ground state are accompanied by emitting characteristic gamma-quanta. The energies of the characteristic emission of different nuclei can be very close to each other. Therefore, not all of them can be distinguished. As a result, they are often fitted by a template (Murphy et al., 2009), varying only the total amplitude. Positrons

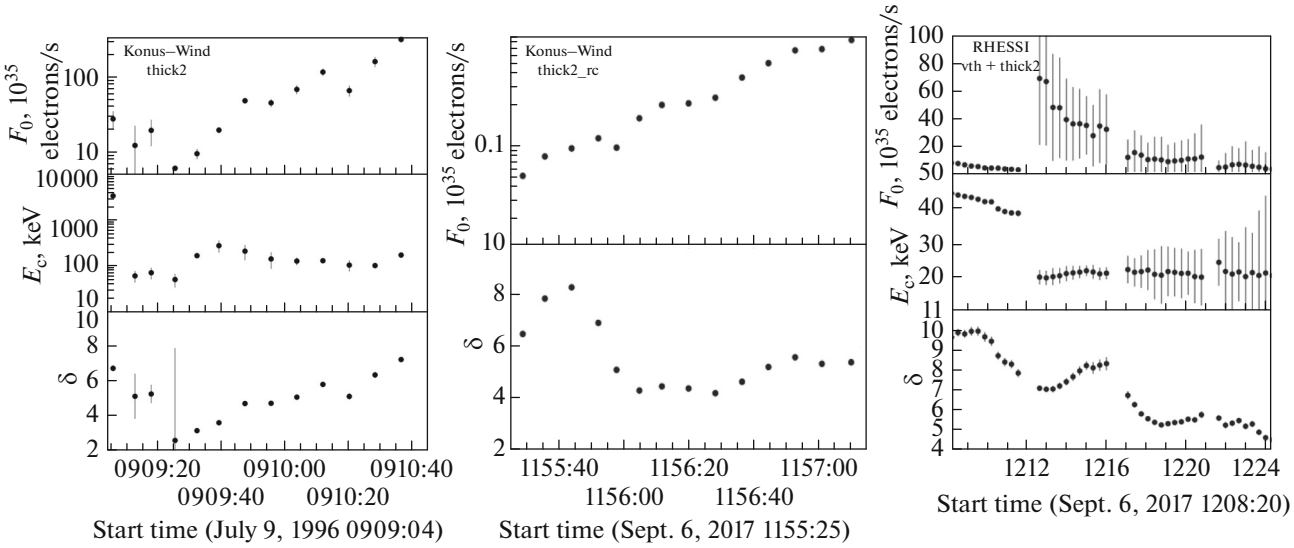

Fig. 5. Evolution of nonthermal parameters (total integral electron flux F_0, low-energy cut-off E_c, spectral index δ of the electron distribution function) obtained from the KW fitting data for the flare SOL1996-07-09T-09:09 (left panel) and from the KW and RHESSI fitting data for the flare SOL2017-09-06T-11:53 (middle and right panels).

born in the reactions also contribute to the radiation continuum, and, when annihilated, give a 511 keV line. The neutrons that are formed as a result of nuclear interactions after slowing down to thermal velocities in the solar photosphere can be captured by protons and give a 2.2 MeV line. The flux in the nuclear deexcitation lines can be used to estimate the number of accelerated protons and the ratio between the flux in the nuclear deexcitation lines and the 2.2 MeV line allows to estimate the spectral index of the accelerated protons (Hua and Lingenfelter, 1987). Based on this, the total energy of accelerated protons can be obtained; the procedure was described in detail by Lysenko et al. (2019). Following Emslie et al. (2012), we estimate the energy of accelerated ions *E-ion* as the triple energy of protons. Figure 6 shows the results of the KW X-ray and gamma-ray spectral fitting for the SOL1996-07-09T-09:09 and SOL2017-09-06T-11:53 flares. For the flare on July 9, 1996, according to the KW data, we obtained $E\text{-}ion = 10 \times 10^{30}$ erg; the energy estimation for the flare on December 13, 2006, was taken from Emslie et al. (2012) and constituted $E\text{-}ion = 14 \times 10^{30}$ erg (Table 1). For the flare of September 6, 2017, the ion energy was taken from Lysenko et al. (2019): $E\text{-}ion = 11 \times 10^{30}$ erg.

3.4. Free Magnetic Energy

To estimate free magnetic energy for the flare on September 6, 2017, coronal magnetic-field extrapolation according to the SDO/HMI data was used in the approximation of a nonlinear, force-free field based on the optimization method (Wheatland et al., 2000). The extrapolation data were provided in Anfinogentov et al. (2019). For the estimations of the free energy of the obtained force-free field a potential field with the same normal component at the boundary of the box as the force-free field was calculated (Rudenko and Anfinogentov, 2017) and the free energy was obtained as the energy difference between the force-free and potential fields and amounted to $E_{magn} = 560 \times 10^{30}$ erg for the flare on September 6, 2017 (Table 1). The free energy corresponding to the flare on December 13, 2006, was previously estimated (Guo and Ding, 2008) and amounted to $E_{magn} = 110 \times 10^{30}$ erg. Unfortunately, for the flare on July 9, 1996, it is impossible to estimate the free energy, because there are no vector magnetograms. Figure 7 shows circular diagrams of the free magnetic energy distribution divided between thermal and nonthermal components.

4. RESULTS AND CONCLUSIONS

In this article, we analyzed the energy of three powerful solar flares during the SA minima with the method proposed by Emslie et al. (2012). For this purpose, we selected three X-class solar flares that occurred in the minima of solar cycles 22–24 and performed spectral analysis of the Konus-Wind and RHESSI data in X- and gamma-ray ranges and the GOES data in SXR range.

It was shown that ion acceleration took place in all three events, which is indicated by the presence of the nuclear deexcitation lines, the line of electron-positron annihilation at 511 keV, and the line of neutron capture by a proton at 2.2 MeV in the gamma-ray spectra. The magnetic free energy, thermal energy,

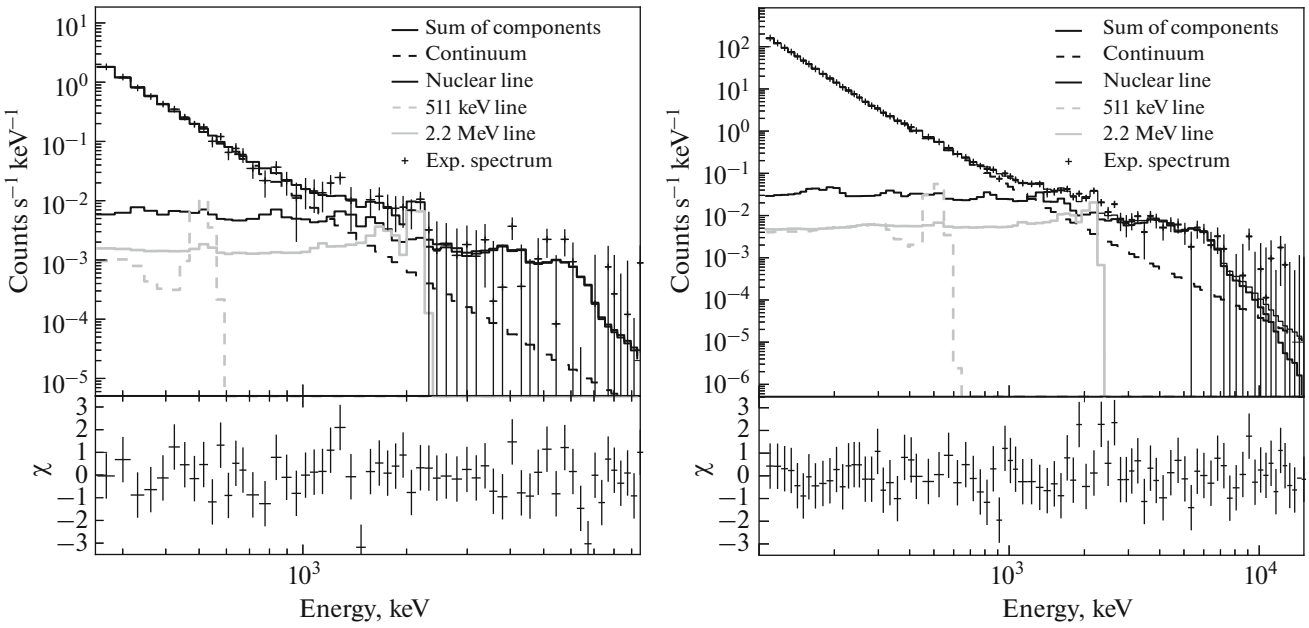

Fig. 6. Left: Fitting results of KW data (crosses) for the flare SOL1996-07-09T-09:09 by four components: power-law model + template for nuclear deexcitation lines + electron-positron annihilation line (511 keV) + 2.2 MeV neutron capture line. Right: Similar to the flare SOL2017-09-06T-11:53, for which the broken power-law function was used instead of the power-law dependence.

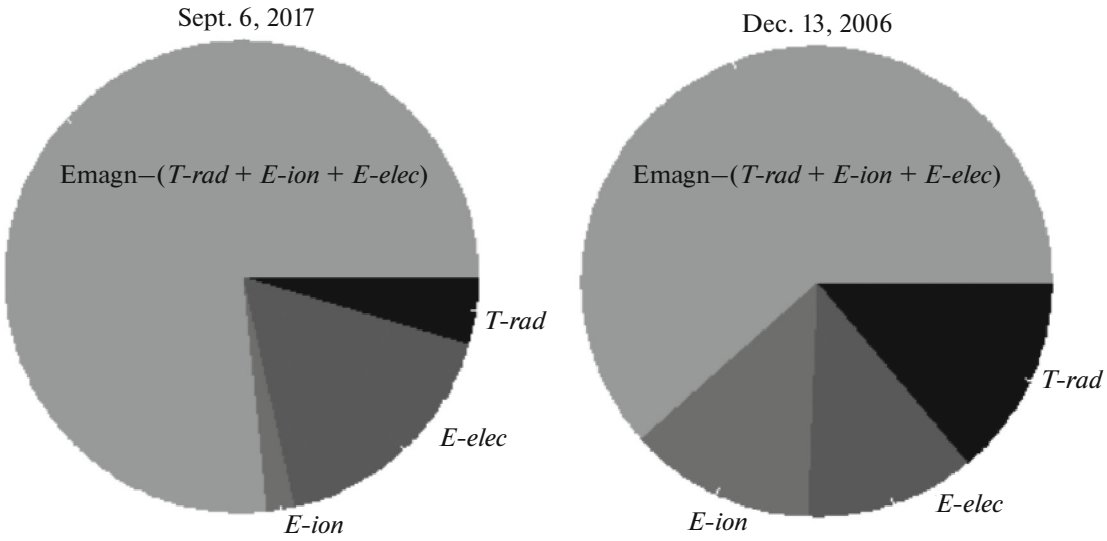

Fig. 7. Distribution of the magnetic free energy (E_{magn}) between thermal energy (*T-rad*), energy of accelerated electrons (*E-elec*), and energy of accelerated ions (*E-ion*) for the events SOL2017-09-06T-11:53 (X9.3) (left panel) and SOL2006-12-13T-10:26 (X3.4) (right panel).

and the energy of accelerated electrons and ions were estimated.

It was shown that the energy of accelerated electrons and ions is larger than thermal energy in all cases: *E-ion*+*E-elec* ~ 19 × *T-rad* for July 9, 1996, *E-ion* + *E-elec* ~1.7 × *T-rad* for December 13, 2006, and *E-ion* + *E-elec* ~ 3.7 × *T-rad* for September 6, 2017. It was also shown in Fig. 7 that a simple scenario in which the entire free magnetic energy is converted into the energy of accelerated particles and direct heating does not work for these events. This indicates that we either underestimate thermal emission (significant emission in ultraviolet range, etc., which is not detected by GOES) or the energy of accelerated particles is converted into kinetic energy, e.g., sunquakes, coronal mass ejections, and solar energetic particles.

We did not find any preferred energy release channel common to all of the studied flares. We hope to consider this question in more detail in the future.

FUNDING

G.G. Motorina and A.L. Lysenko acknowledge the support of the Russian Foundation for Basic Research, project no. mol_a 18-32-00439. G.G. Motorina also acknowledges the project RVO:67985815 and the project LM2015067: EU-ARC.CZ—National Research Infrastructure by Ministry of Education of the Czech Republic. G.D. Fleishman acknowledges the support of NSF grant AGS-1817277 and NASA grants 80NSSC18K0667, 80NSSC19K0068, 80NSSC18K1128, and 80NSSC20K0627. S.A. Anfinogentov acknowledges the support of the Basic Research Program II.16 and the Russian Foundation for Basic Research, project no. 19-52-53045.

CONFLICT OF INTEREST

The authors declare that they have no conflict of interest.

REFERENCES

Anfinogentov, S.A., Stupishin, A.G., Mysh'yakov, I.I., and Fleishman, G.D., Record-breaking coronal magnetic field in solar active region 12673, *Astrophys. J. Lett.*, 2019, vol. 880, no. 2, id L29.

Aptekar, R.L., Frederiks, D.D., Golenetskii, S.V., et al., Konus-W gamma-ray burst experiment for the GGS Wind Spacecraft, *Space Sci. Rev.*, 1995, vol. 71, pp. 265–272.

Brown, J.C., The deduction of energy spectra of non-thermal electrons in flares from the observed dynamic spectra of hard X-ray bursts, *Sol. Phys.*, 1971, vol. 18, no. 3, pp. 489–502.

Emslie, A.G., Dennis, B.R., Shih, A.Y., et al., Global energetics of thirty-eight large solar eruptive events, *Astrophys. J.*, 2012, vol. 759, id 1.

Gary, D.E., Chen, B., Dennis, B.R., et al., Microwave and hard X-ray observations of the 2017 September 10 solar limb flare, *Astrophys. J.*, 2018, vol. 863, id 83.

Guo, Y. and Ding, M.D., 3D magnetic field configuration of the 2006 December 13 flare extrapolated with the optimization method, *Astrophys. J.*, 2008, vol. 679, pp. 1629–1635.

Hathaway, D.H., The solar cycle, *Living Rev. Sol. Phys.*, 2015, vol. 12, no. 1, id 4.

Hua, X.M. and Lingenfelter, R.E., Solar flare neutron production and the angular dependence of the capture gamma-ray emission, *Sol. Phys.*, 1987, vol. 107, no. 2, pp. 351–383.

Knipp, D.J., Ramsay, A.C., Beard, E.D., et al., The May 1967 great storm and radio disruption event: Extreme space weather and extraordinary responses, *Space Weather*, 2016, vol. 14, no. 9, pp. 614–633.

Kosovichev, A.G. and Zharkova, V.V., X-ray flare sparks quake inside sun, *Nature*, 1998, vol. 393, no. 6683, pp. 317–318.

Lin, R.P., Dennis, B.R., Hurford, G.J., et al., The Reuven Ramaty High-Energy Solar Spectroscopic Imager (RHESSI), *Sol. Phys.*, 2002, vol. 210, no. 1, pp. 3–32.

Lysenko, A.L., Anfinogentov, S.A., Svinkin, D.S., Frederiks, D.D., and Fleishman, G.D., Gamma-ray emission from the impulsive phase of the 2017 September 6 X9.3 flare, *Astrophys. J.*, 2019, vol. 877, no. 2, id 145.

Mewaldt, R.A., Leske, R.A., Stone, E.C., et al., STEREO observations of energetic neutral hydrogen atoms during the 2006 December 5 solar flare, *Astrophys. J. Lett.*, 2009, vol. 693, no. 1, pp. L11–L15.

Meyer, P., Parker, E.N., and Simpson, J.A., Solar cosmic rays of February 1956 and their propagation through interplanetary space, *Phys. Rev.*, 1956, vol. 104, no. 3, pp. 768–783.

Murphy, R.J., Kozlovsky, B., Kiener, J., and Share, G.H., Nuclear gamma-ray de-excitation lines and continuum from accelerated-particle interactions in solar flares, *Astrophys. J. Suppl. Ser.*, 2009, vol. 183, no. 1, pp. 142–155.

Omodei, N., Pesce-Rollins, M., Longo, F., Allafort, A., and Krucker, S., Fermi-LAT observations of the 2017 September 10 solar flare, *Astrophys. J. Lett.*, 2018, vol. 865, id L7.

Ramaty, R., Kozlovsky, B., and Lingenfelter, R.E., Solar gamma rays, *Space Sci. Rev.*, 1975, vol. 18, no. 3, pp. 341–388.

Raymond, J.C., Cox, D.P., and Smith, B.W., Radiative cooling of a low-density plasma, *Astrophys. J.*, 1976, vol. 204, pp. 290–292.

Rudenko, G.V. and Anfinogentov, S.A., Algorithms of the potential field calculation in a three-dimensional box, *Sol. Phys.*, 2017, vol. 292, no. 8, id 103.

Solanki, S.K., Usoskin, I.G., Kromer, B., et al., Unusual activity of the Sun during recent decades compared to the previous 11,000 years, *Nature*, 2004, vol. 431, no. 7012, pp. 1084–1087.

Syrovatskii, S.I. and Shmeleva, O.P., Plasma heating by fast electrons and nonthermal X-ray radiation during solar flares, *Astron. Zh.*, 1972, vol. 49, pp. 334–347.

Vilmer, N., Mackinnon, A.L., and Hurford, G.J., Properties of energetic ions in the solar atmosphere from γ-ray and neutron observations, *Space Sci. Rev.*, 2011, vol. 159, nos. 1–4, pp. 167–224.

Wheatland, M.S., Sturrock, P.A., and Roumeliotis, G., An optimization approach to reconstructing force-free fields, *Astrophys. J.*, 2000, vol. 540, no. 2, pp. 1150–1155.

White, S.M., Thomas, R.J., and Schwartz, R.A., Updated expressions for determining temperatures and emission measures from GOES soft S-ray measurements, *Sol. Phys.*, 2005, vol. 227, no. 2, pp. 231–248.

Yang, S., Zhang, J., Zhu, X., and Song, Q., Block-induced complex structures building the flare-productive solar active region 12673, *Astrophys. J. Lett.*, 2017, vol. 849, no. 2, id L21.

Zharkova, V.V. and Gordovskyy, M., The kinetic effects of electron beam precipitation and resulting hard X-ray intensity in solar flares, *Astron. Astrophys.*, 2005, vol. 432, no. 3, pp. 1033–1047.

Translated by O. Pismenov